

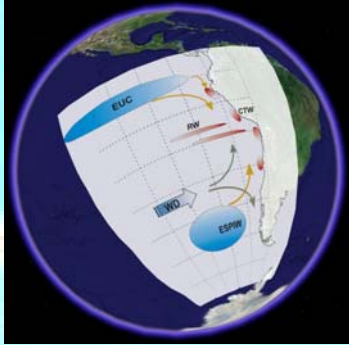


The seasonal cycle of the oxygen minimum zone and the extra-tropical Rossby wave in the South Eastern Pacific



Boris Dewitte (1), Oscar Pizarro (3,4), Vincent Echevin (2), and Yves duPenhoat (1)
(1) LEGOS/IRD-Toulouse, (2) LOCEAN/IRD-Paris, (3) PROFCO/COPAS-UDEC-Concepción (4) DGEU-UDEC-Concepción

Abstract: The seasonal cycle of the OMZ in the southern Pacific is documented from the World Ocean Atlas 2001 (WOA01F). The focus is on the annual harmonic of the low O_2 concentration. The largest amplitudes are found in the surroundings regions of the limits of the OMZ although some latitudinal variability is observed. South of 20°S, the maximum variability is concentrated near the coast whereas, north of 15°S, it is located off-shore. In between, the variability is weak reflecting the observed low kinetic energy of this region. Observed winds (ERS), hydrographic data, altimetry (TOPEX/POSEIDON) and the outputs of medium-resolution general circulation model are used to document the large-scale ocean dynamics in the region at seasonal timescale. In particular, the variability associated to the extra-tropical Rossby wave is analysed. Assuming O_2 concentration as a passive tracer, an estimation of the transport of O_2 by the annual Rossby wave contribution to the zonal current is derived. In the light of the results, it is suggested that the seasonal westward expansion of the OMZ is to some extent associated to the advection of low O_2 concentration by the extra-tropical Rossby waves.



Mean characteristics of the South Eastern Pacific: The Humboldt Current is characterized by the existence of an Oxygen Minimum Zone (OMZ). The OMZ is embedded in the complex Eastern South Pacific Current System. On the large scale this system is fed from all sides: the South, the North and the off-shore ocean. A rough representation of the water mass influx is the following: large scale intermediate water masses (Antarctic Intermediate Water -AAIW- and Eastern South Pacific Intermediate Water -ESPIW-) penetrate from the south into the ESP. The ESPIW deepens westward and northward from its outcrop region (around 32°S) reaching 150 m depth. To the North, the equatorial undercurrent brings cold waters feeding the poleward Peru-Chile Undercurrent along the coast of the ESP. To the west, the large scale atmospheric gyre brings waters from the off-shore ocean at around -40°S. This surface waters split in a northward and southward branches as it arrives close to the Chilean coast. The eastern branch of this surface anticyclonic circulation forms the northward Chile-Peru Current. Closer to the coast, a strong off-shore current shear exists that is not discernible from altimetric data because of the rather fine off-shore scale (~200 km): i) The CCC (Chile Coastal Current) and the Peru Coastal Current (PCC) flows northward (Strub et al. 1998) in the near surface layers (0-100 m, 20 cm s⁻¹), with a 100 km width, and its maximum is located at the level of the thermal front generated by the upwelling of cooler water at the coast. Its intensity is maximum in spring and in summer when equatorward winds are strongest off central Chile. This current transports highly oxygenated surface waters from the south. ii) The PCCC (Peru-Chile Counter Current), a southward surface current, was observed offshore, 100-300 km from the coast (Strub et al. 1995, 1998). Processes explaining the dynamics of this counter-current, of direction opposed to the density gradient, are still badly known. The wind curl could force the current southwards, in agreement with Sverdrup dynamics (Strub et al. 1998). The potential role of this current in advecting poorly oxygenated waters from the equatorial area is unknown. iii) More offshore, the southern branch of the anticyclonic subtropical gyre of the south-eastern Pacific, named the South Pacific Current, flows towards the American coast between 35°S and 48°S. It then separates in two branches, one directed to the north, forming the Chile-Peru or Humboldt Current, a relatively broad (1500 km), deep (700-1000 m) and weak current (5-10 cm s⁻¹). The Chile-Peru Current, which seems to delimit the western boundary of the OMZ, feeds the South Equatorial Current and also participates to an anticyclonic recirculation cell. iv) The Peru-Chile Undercurrent (PCU) is a well-defined, poleward, subsurface flow, which extends over the continental shelf and slope off the west coast of South America with a core located between 100 and 300 m depth.



Figure 1: Schematics of the dominant oceanographic features in the South Eastern Pacific. The picture on the right hand side show the same schematics with the OMZ superimposed (green dots). Data are from the World Ocean Atlas 2001 (annual mean, z=300m and 400m).

(EUC: Equatorial Under Current, CTW: Coastal Trapped Wave, RW: Rossby wave, WD: Western Drift, ESIPIW: Eastern South Pacific Intermediate Water)

Oceanic variability:

Superimposed to the mean circulation, the SEP is characterized by a large variability at a broad band of frequencies. First of all, as an extension of the equatorial wave guide, the coastal circulation is under the direct influence of the tropical variability, which includes ENSO (El Niño Southern Oscillation). Atmospheric waves trapped by the Andes chain propagate southward at a speed of approximately 900 km/day and locally force nearshore oceanic variability at 5 to 10 days time-scale (Shaffer et al. 1997). At lower frequency, oceanic equatorial Kelvin waves transmit part of their energy to coastal waves when they reach the South American coast. Coastal waves trapped by topography (Brink, 1982) propagate poleward at 3 m s⁻¹ (Shaffer et al. 1997, Ulloa et al. 2001), at distances reaching 15000 km. They induce a 50-day variability which influences the undercurrent flow and vertical structure, managing to reverse the PCU flow northward at certain periods (Shaffer et al. 1997). In addition they induce vertical displacements of the thermocline and nutricline, which involve fluctuations of temperature and of primary and secondary productivities (Ulloa et al. 2001). This intraseasonal variability is reinforced during El Niño periods, when equatorial Kelvin waves are more frequent and intense, and the thermocline is deeper.

On interannual and seasonal scales, poleward propagation of sea level anomalies at speeds varying between 0.4 and 0.9 m s⁻¹ was observed. On its passage, this signal generates westward propagation of Rossby waves (Vega et al. 2003; Ramos et al. 2006). Thus, there is a strong dynamical coupling between variability in the tropics and along the Peru-Chile coasts, at interannual and seasonal timescales. At higher frequencies, the important semiannual variability presented by the PCU near 30°S has been also related to equatorial Kelvin waves reaching the South American coast (Pizarro et al., 2002). The annual component of the Undercurrent variability is related to the alongshore wind stress integral. Recently Ramos et al. (2006) analysed the seasonal cycle of the thermocline depth off Chile and demonstrate that it associated to a large extent to the propagation of the Rossby waves.

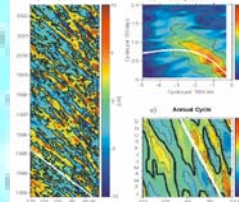


Figure 2: a) Longitude-time diagram of the SLH anomalies at 21°S from TP/ERS data. The white line represents the theoretical phase speed for first vertical mode of a long Rossby wave. b) 2-D spectrum for the data in the panel a. The line in the spectrum is the theoretical dispersion curve for the first mode of baroclinic Rossby wave. c) Longitude-time diagram of the seasonal cycle of the SLH anomalies estimated from data in the panel a. The white line also represents the theoretical phase speed for first vertical mode of a long Rossby wave (After Ramos et al. (2006))

OMZ annual variability:

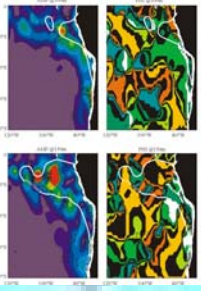


Figure 3: Maps of the amplitude and phase of the OMZ annual harmonic at 100m (top) and 150m (bottom). The thick white line correspond to the mean position of the $O_2=1$ mL/L iso-line.

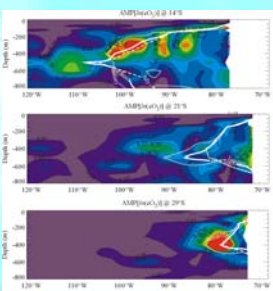


Figure 4: Longitude-depth sections of the OMZ $[-\ln(O_2+1-c_{omz})]$ at 14°S, 21°S and 29°S. The thick white line correspond to the mean position of the $O_2=1$ mL/L iso-line, where the dotted and dashed line correspond to the January and July location respectively.

The seasonal Rossby wave and the ZMO:

In order to focus on the low O_2 concentration, $-\ln(O_2+1-c_{omz})$ is analyzed instead of O_2-c_{omz} is equal to 1 ml/l in this study.

Figures 3 and 4 indicate that the amplitude of the annual cycle of the OMZ is maximum in the surroundings of its limit ($O_2=1$ mL/L), namely in the upper 200m in the northern part of the domain (0°-10°S) and deeper and closer to the coast south of 10°S. At 29°S, it peaks at (480m-80°W). The annual cycle of the OMZ corresponds to a large extent to a longitudinal extension of its limit as evidenced by the positions of the $O_2=1$ mL/L iso-line for January and July on figure 4

The inner domain of the OMZ is characterised by a relative maximum amplitude of the annual cycle of the sea level (figure 5a). Inside this domain, the annual cycle of sea level propagate off-shore as extra-tropical Rossby wave as suggested by the phase lines (figure 5b). The latitudinal variability of the sea level amplitude and phase line configuration is characteristic of the change in phase speed of the theoretical Rossby waves as function of longitude. Near the OMZ limit, the amplitude of the geostrophic zonal currents as observed by the TOPEX/POSEIDON satellite (figure 5c) is maximum, suggesting that the extra-tropical Rossby wave transport the low O_2 concentration off-shore.

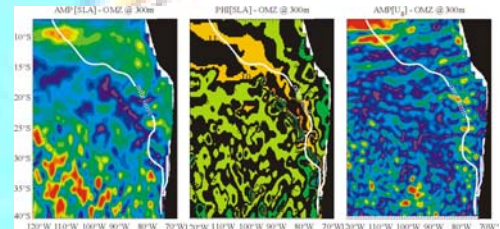


Figure 5: Maps of the amplitude and phase (annual harmonic) of TOPEX/POSEIDON sea level anomalies (units is cm, red correspond to -2 cm). The amplitude of the annual harmonic of the corresponding geostrophic zonal currents is displayed on the right panel (unit is cm/s, red corresponds to 50 cm/s). The thick white line correspond to the mean position of the $O_2=1$ mL/L iso-line at 300 m.

Advection of the OMZ by the extra-tropical Rossby wave:

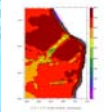
Considering the above, the hypothesis that is aimed to be tested in this study is to estimate to which extent the seasonal cycle of the OMZ can be explained by the off-shore advection of low O_2 concentration by the annual extra-tropical Rossby wave. In other word, to which extent, the following equation is valid:

$$\frac{d(\ln(O_2+1-c_{omz}))}{dt} = -u \frac{d(\ln(O_2+1-c_{omz}))}{dx}$$

A combination of model simulation and observation is used to test the hypothesis. The model simulation consists in a seasonal run of a medium-resolution regional ocean general circulation model. A vertical mode decomposition of the model is performed in order to derive the propagating seasonal variability (first mode contribution) of the off-shore current and derive the vertical mode structure of the first baroclinic mode as a function of space. The latter is used to infer the observed geostrophic current at a particular depth and derive the transport of low O_2 concentration in the core of the OMZ.

Model setup:

- climatological run (P4):
- Boundary conditions: ORCA (2°x0.5°) monthly climatology from a 1992-1998 run
- data (T,S,U,V) averaged
- regional model atmospheric forcing: ERS winds, NCEP heat fluxes, CMAP precipitation fluxes
- regional model resolution: 1/3°x1/3°



Regional model topography and domain.

Vertical mode decomposition of the model variability:

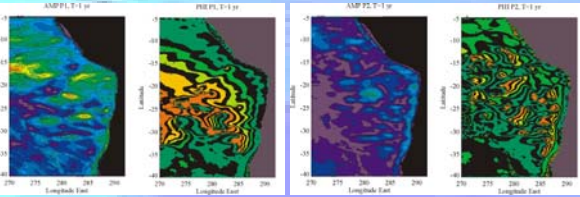


Figure 6: Maps of the annual harmonic of the first (left) and second (right) baroclinic mode contributions to sea level anomalies, a) amplitude (in cm) and b) phase (label '1' corresponds to January)

The results indicate that a significant part of the variability projects on the first and second baroclinic modes at seasonal and intraseasonal timescales. At annual timescale, whereas the first baroclinic mode contribution variability extends far off shore for the first modes, it is more concentrated near the coast for the second baroclinic mode.

The annual cycle of the first baroclinic mode contribution to sea level anomalies exhibits a clear off-shore propagation with the phase lines of the 1-yr harmonic parallel to each others over most of the basin. For the second baroclinic mode, the off-shore propagations are more confined near the coast where the amplitude of the annual harmonic is the largest. Off-shore, propagations can be seen but they are more erratic with phase speed that does not decrease with latitude.

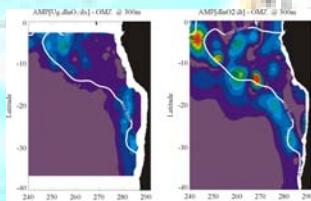


Figure 6: Maps of the amplitude of the annual cycle of the rate of change in $-\ln(O_2+1-c_{omz})$ (left) and the zonal advection of $-\ln(O_2+1-c_{omz})$ by the geostrophic current as derived from the TOPEX/POSEIDON sea level anomalies at 300m. Unit is $\ln(\text{mL/L}) \text{ days}^{-1}$. Contour interval is every 4 units. The thick white line corresponds to the mean position of the $O_2=1$ mL/L iso-line.

To estimate the zonal advection of the low O_2 content, the geostrophic currents as derived from TOPEX/POSEIDON sea level anomaly are used assuming that they are representative of the first baroclinic mode. The results are displayed in figure 6 along with the rate of change in low O_2 content. Interestingly, the amplitude of the signals are comparable, somewhat lower by ~20% for the advection term. The zonal advection is the largest south of -18°S and north of -12°S. Similar calculation are performed using the model currents and the results of the vertical mode decomposition. This allows in particular to estimate the transport associated to the first two baroclinic mode and to take into account the heterogeneity of the density field (through the vertical mode structure functions). Note that the model currents are weaker than the observations so that a coefficient (10) was applied to get comparable amplitude of the advection terms and the rate of change of $-\ln(O_2+1-c_{omz})$. The results indicate that the first baroclinic mode is the main contributor to the transport of low O_2 content in the southern part of the domain. At 400 m the amplitude of the rate of change in O_2 is maximum near (78°W, 29°S) like for the advection terms.

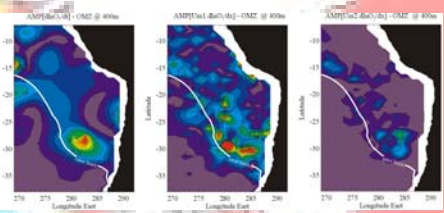


Figure 7: similar to figure 6 but at 400 m and for the advection terms as derived from the model climatological zonal current for the first and second baroclinic modes. The advection terms were multiplied by 10. Compared to figure 6.

Conclusions: The OMZ encompasses a zone of maximum variability of the annual cycle of the sea level anomaly. Its annual cycle is also characterized at the large scale by a maximum variability in zonal current annual cycle, namely far off shore in the tropics and closer to the coast with increasing latitude. This suggests that the extension of the OMZ at seasonal cycle may be due to the zonal transport of low O_2 content by the annual extra-tropical Rossby wave. A rough estimate of this transport from observation leads to comparable amplitude for zonal advection of low O_2 content by the geostrophic currents and the rate of change of the low O_2 content. Estimate of this transport from regional model outputs confirms the dominance of the first baroclinic mode contribution for advecting water property. The flaws of the model (mostly underestimation of the current and sea level seasonal variability) do not allow to conclude at a major role of the ocean dynamics in explaining the seasonal cycle of the OMZ in the South Eastern Pacific.

References:
-Pizarro, O., Shaffer, G., Dewitte, B., Ramos, M., 2002. Dynamics of seasonal and interannual variability of the Peru-Chile Undercurrent. *Geophysical Research Letters* 29, 22-1/22-4.
-Ramos M., O. Pizarro, L. Bravo and B. Dewitte, 2006. Seasonal variability of the permanent thermocline off northern Chile. *Geophys. Res. Lett.*, in press.
-Shaffer, G., O. Pizarro, L. Durlfield, S. Salinas, and J. Rutant, 1997. Circulation and low frequency variability near the Chile coast: remotely-forced fluctuations during the 1991-1992 El Niño. *J. Phys. Oceanogr.*, 27, 217-235.
-Strub, P.T., J. M. Masias and C. James, 1995. Altimeter observations of the Peru-Chile counter-current. *Geophys. Res. Lett.*, 2(3), 211-214, 1995.
-Simp, P.T., J. M. Masias, V. Montecino, J. Rutant and S. Salinas, 1998. Coastal ocean circulation off western south America. In: The sea, regional studies and synthesis. Robinson & Brink (Eds.), 11. Wiley & Sons, 1998.
-Ulloa, O., R. Escobar, S. Homazabal, R. A. Quiñones, R. R. González & M. Ramos. Evolution and biological effects of the 1997-98 El Niño in the upwelling ecosystem off northern Chile. *Geophysical Research Letters*, 28, 1591-1594, 2001.
-Vega, A., duPenhoat, Y., Dewitte, B., and O. Pizarro, 2003. Equatorial forcing of interannual Rossby waves in the eastern South Pacific. *Geophysical Research Letters*. DOI: 10.1029/2002GL015886.
Acknowledgements: The preparation and development of this work were made possible thanks to several states funded by ECOS (grants NC C3U06) of Y. duPenhoat, B. Dewitte, O. Pizarro at PROFCO and LEGOS.